Article

Manganese Mediates its Antiviral Functions in a cGAS-STING Pathway Independent Manner

Shaohua Sun [1,2,3,4], Yulin Xu [1,2,3,4], Ming Qiu [1,2,3,4], Sen Jiang [1,2,3,4], Qi Cao [1,2,3,4], Jia Luo [1,2,3,4], Tangjie Zhang[1,2,3,4], Nanhua Chen [1,2,3,4], Wanglong Zheng [1,2,3,4], Francois Meurens [5,6], Zongping Liu [1,2,3,4]*, Jianzhong Zhu [1,2,3,4]*

1 College Veterinary Medicine,
2 Joint International Research Laboratory of Agriculture and Agri-Product Safety,
3 Comparative Medicine Research Institute,
4 Jiangsu Co-innovation Center for Prevention and Control of Important Animal Infectious Diseases and Zoonoses, Yangzhou University, Yangzhou, 225009, P R China;
5 Swine and Poultry Infectious Diseases Research Center, Faculty of Veterinary Medicine, University of Montreal, St-Hyacinthe, QC, Canada J2S 2M2;
6 Department of Veterinary Microbiology and Immunology, Western College of Veterinary Medicine, University of Saskatchewan, Saskatoon, SK, Canada S7N 5E2
* Correspondence: to liuzongping@yzu.edu.cn (Z.L.) and jzzhu@yzu.edu.cn (J.Z.)

Abstract: The innate immune system is the first line of host defense sensing viral infection. Manganese (Mn) has recently been found to be involved in the activation of innate immune DNA sensing cGAS-STING pathway and subsequent anti-DNA virus function. However, whether Mn^{2+} mediates host defense against RNA viruses is still unclear. In the current study, we demonstrated that Mn^{2+} exhibited antiviral effects against various animal and human viruses including RNA viruses such as PRRSVs and the VSV as well as a DNA virus such as the HSV1 in a dose-dependent manner. Moreover, cGAS and STING were both investigated in the Mn^{2+} mediated antiviral roles using the knockout cells made by CRISPR-Cas9 approach. Unexpectedly, the results revealed that neither cGAS knockout nor STING knockout had any effect on Mn^{2+} mediated antiviral functions. Nevertheless, we verified that Mn^{2+} promoted the activation of cGAS-STING signaling pathway. These findings suggest that Mn^{2+} has broad spectrum antiviral activities in a cGAS-STING pathway independent manner. This study also provides significant insights into redundant mechanisms participating in the Mn^{2+} antiviral functions and also indicates new target for Mn^{2+} antiviral therapeutics.

Keywords: manganese; cGAS-STING pathway; RNA virus; antiviral function; redundant mechanisms

1. Introduction

The innate immune system is the first line of host defense against multiple danger signals from pathogens or cellular damage. It encodes various host germline-encoded pattern recognition receptors (PRRs), which recognize pathogen-associated molecular patterns (PAMPs) and damage associated molecular patterns (DAMPs)[1, 2]. To fight infection and achieve homeostasis, the PRRs cause the activation of gene transcription or protease-dependent cytokine maturation, producing antiviral interferons (IFNs), proinflammatory cytokines, and chemokines [1, 2]. Host antiviral innate immune responses are elicited during viral infections, and upon engagement by viral infections, cells use different PRRs to sense viral nucleic acids [3]. DNA sensing PRRs are Toll-like receptor 9 (TLR9), cyclic GMP-AMP synthase (cGAS), stimulator of interferon genes (STING), absent in melanoma 2 (AIM2), and interferon gamma-inducible 16 (IFI16) [4]. RNA sensing PRRs include endosomal TLR3, TLR7, TLR8, and cytosolic retinoic acid inducible gene-I (RIG-I), melanoma differentiation-associated gene 5 (MDA5), NOD-like receptor pyrin domain containing 3 (NLRP3) and nucleotide-binding and oligomerization domain containing 2 (NOD2) [5].

The cGAS-STING pathway has been identified to be the important DNA-sensing machinery in innate immunity, against pathogen aggresion [6, 7]. cGAS senses the presence of non-self and self DNA, and utilizes substrates ATP and GTP to catalyze the production of the second messenger cyclic GMP-AMP (2′3′-cGAMP) that then activates the signaling adaptor protein STING [6, 7]. Activated STING recruits the downstream TANK-binding kinase 1 (TBK1) and TBK1 is auto-phosphorylated [6, 8]. Then, the transcription factor IRF3, which is recruited by STING and phosphorylated by TBK1, translocates to the nucleus and induces antiviral type I IFNs and IFN stimulated genes (ISGs) [6, 8]. Another transcription factor NF-κB is also activated by STING-TBK1 signaling and drives proinflammatory gene expressions [6, 9].

Manganese (Mn) is required as an enzymatic cofactor in many physiologic processes, such as protein and energy metabolism, immune function, development, reproduction, neuronal regulation, and antioxidant defenses [10-12]. Several canonical signaling pathways have been reported to be Mn-responsive, including ataxia telangiectasia mutated 2 (ATM), p53, phosphatidylinositol 3 kinase (PI3K), insulin and insulin-like growth factor-1 (IGF-1) pathways [13-15]. However, attention has been recently paid to the Mn in the regulation of cGAS-STING pathway, which exert a potent host defense against DNA viruses [16]. Mn^{2+} was shown to increase the sensitivity of cGAS to double-stranded DNA (dsDNA) and its enzymatic activity. It also facilitates STING activity by boosting cGAMP-STING binding affinity [16]. Further studies have revealed that Mn^{2+} directly activated cGAS to induce a noncanonical catalytic synthesis of 2′3′-cGAMP, through similar overall conformation to dsDNA-activated cGAS [17, 18].

Interestingly, recent publications have suggested the relevance of the cGAS-STING pathway in the process of RNA virus infections [19-22]. However, whether Mn^{2+} plays a role in the cGAS-STING pathway mediated anti-RNA virus infections is still largely unclear. Moreover, how the Mn^{2+} mediates its antiviral functions is not fully elucidated. In the current study, we found that Mn^{2+} exerts a broad antiviral functions against various viruses including some RNA and DNA viruses, which is independent on the cGAS-STING pathway.

2. Materials and methods

2.1. Cells and viruses

Marc-145 cells and HEK293T cells were cultured in DMEM (HyClone Laboratories, Logan, UT, USA) containing 10% fetal bovine serum (FBS) and 1% penicillin-streptomycin solution at 37 °C with 5% CO_2. Porcine alveolar macrophages (3D4/21, ATCC CRL-2843) were grown in RPMI 1640 (Hyclone Laboratories, Logan, UT, USA) supplemented with 10% FBS with 1% penicillin–streptomycin solution, and maintained at 37 °C with 5% CO_2 in a humidified incubator. The viruses including a DNA virus Herpes Simplex Virus 1 (HSV1-GFP) as well as RNA viruses Vesicular Stomatitis Virus (VSV-GFP) and Highly Pathogenic Porcine Reproductive and Respiratory Syndrome Viruses (HP-PRRSV XJ17-5-GFP and HP-PRRSV vaccine strain JXA1-R-GFP) were used as we previously reported [22-24].

2.2. Cell treatments

The Marc-145 cells were pretreated with different concentrations of Mn^{2+} ($MnCl_2 \cdot 4H_2O$) (Sigma-Aldrich, St. Louis, MO, USA) for 24 h and then infected with 0.1 multiplicity of infection (MOI) PRRSV XJ17-5 or JXA1-R. The 3D4/21 cells were also pretreated with Mn^{2+} ($MnCl_2 \cdot 4H_2O$) for 24 h, and subsequently infected with 0.01 MOI HSV-1 or 0.001 MOI VSV. Additionally, 3D4/21 cells were transfected with cGAS agonist poly dA:dT (InvivoGen, Hong Kong, China) or STING agonist 2′3′-cGAMP (InvivoGen, Hong Kong, China) by using the transfection reagent Lipofectamine 2000 (ThermoFisher Scientific, Shanghai, China) and then exposed to Mn^{2+} treatment for 24 h.

2.3. Western blot analysis

Proteins were extracted in radioimmunoprecipitation assay (RIPA) lysis buffer, mixed with 4 × loading buffer by 3:1 ratio, and boiled at 100°C for 5-10 min. The protein samples were separated on 10% SDS-PAGE gels, and then transferred to PVDF membranes. After blocking with 5% skim milk solution at room temperature (RT) for 60 min, membranes were incubated with individual primary antibodies at 4 °C overnight. The primary antibodies include anti-GFP (HT801-01, TransGen, Beijing, China), STING (19851-1-AP, ProteinTech, Wuhan, China), cGAS (sc-515777, Santa Cruz Biotechnology, Dallas, Texas, USA), IRF3 (11904S, CST, Boston, MA, USA), p-IRF3 (Ser396) (MA5-14947, ThermoFisher Scientific, Shanghai, China), TBK1 (3504S, CST, Boston, MA, USA), p-TBK1 (5483S, CST, Boston, MA, USA) and β-actin (5057, CST, Boston, MA, USA). Secondary antibody HRP-conjugated goat anti-mouse or rabbit IgG (Transgen Biotech, Beijing, China) was used to incubate with the membranes for 60 min at RT. Signals were detected using enhanced chemiluminescence (ECL) substrate (Tanon, Shanghai, China) and images were visualized by imaging system (Tanon, Shanghai, China).

2.4. Quantitative reverse transcription polymerase chain reaction (qRT-PCR)

Total RNA was extracted using TRIpure reagent (Aidlab, Beijing, China). The cDNA was synthesized using HiScript® 1st Strand cDNA Synthesis Kit (Vazyme, Nanjing, China). The target gene expressions were examined using ChamQ Universal SYBR qPCR Master Mix (Vazyme, Nanjing, China) on a StepOne Plus real-time PCR system (Applied Biosystems, Foster City, CA, USA). The qPCR program was 95 °C for 30 s, followed by 40 cycles of 95 °C for 5 s and 60 °C for 1 min. β-actin served as an internal reference control. The relative mRNA levels were calculated using $2^{-\Delta\Delta CT}$ method. For all the qPCR assays, an efficiency comprised between 90 and 110% was measured. The sequence of qPCR primers used in this study were listed in Table S1.

2.5. CRISPR gRNA design and preparation of Knockout (KO) cells

The CRISPR gRNAs targeting porcine cGAS and monkey cGAS were designed using the web tool from Benchling (www.benchling.com). For each gene, two gRNAs were chosen according to the predicted high scores, respectively, which are shown in Table S2. The recombinant pX458-gRNA plasmids were obtained when the annealed gRNA encoding DNA sequences were cloned into the *Bbs* I site of pX458-EGFP. Marc-145 cells or 3D4/21 cells were transfected with the corresponding recombinant pX458-gRNA plasmids using Lipofectamine 2000. At 24 h post transfection, the GFP positive cells were sorted by a FACS Aria SORP cell sorter (Becton Dickinson) and cultured in 96-well plates by limiting dilution for monoclonal growth. The individual cell clones were screened by PCR using primers shown in Table S2. Briefly, the genomic PCR products were cloned into T vector with pClone007 versatile simple vector kit (TsingKe Biological Technology, Beijing, China). Base substitution, insertion and deletion (ins/del) mutations were analyzed after the sequencing of inserted fragments, and $cGAS^{-/-}$ monkey Marc-145 cells and $cGAS^{-/-}$ porcine macrophages (3D4/21) were each acquired (Fig. S1). In addition, the $STING^{-/-}$ Marc-145 cells and $STING^{-/-}$ 3D4/21 cells were previously obtained and have been used in our lab [22, 25].

2.6. Virus tissue culture infectious dose 50 (TCID50) titrations

Marc-145 cells or 3D4/21 cells were seeded into 96-well plates, and then infected with 10-fold serial dilutions of various virus samples (Marc-145 cells for PRRSVs and 3D4/21 cells for VSV and HSV1). Next, the infected cell supernatants were replaced with fresh DMEM or RPMI 1640 containing 2% FBS, and the cells were monitored for the GFP fluorescence and cytopathic effects (CPE) characterized by cell clumping and shrinkage in Marc-145 cells or 3D4/21 cells after infections for 1-5 days. Finally, the viral titers were expressed as TCID50 and calculated using the method of Reed-Muench.

2.7. Dual-luciferase reporter promoter assay

293T cells were seeded in 96-well plates followed by transfection at next day. Cells were co-transfected with reporter plasmids, ISRE-Firefly luc (Fluc) or IFNβ-Fluc (10 ng/well) and *Renilla* luciferase (Rluc) reporters (0.2 ng/well), plus the indicated porcine cGAS and STING plasmids or vector control (10-30 ng/well) using Lipofectamine 2000. The total DNA per well was normalized with control vectors to 50 ng. Twenty-four hours post transfection, cells were treated with different concentrations of Mn^{2+} for another 24 h. Then, cells were harvested and luciferase activities were detected with the TransDetect Double-Luciferase Reporter Assay Kit (Vazyme, Nanjing, Jiangsu, China). The fold changes were calculated relative to control samples after Fluc normalization by corresponding Rluc.

2.8. Statistical analysis

The results were analyzed using the software GraphPad Prism 6.0 and expressed as the mean ± standard deviation (SD). Statistical analysis was conducted by one way ANOVA followed by Tukey's post hoc test. The normality of the data distribution was assessed using Shapiro-Wilk test. The p value less than 0.05 was considered statistically significant.

3. Results

3.1. Mn^{2+} exerted antiviral functions against PRRSV, VSV and HSV-1

To investigate the effect of Mn^{2+} on the different viruses, Marc-145 cells and 3D4/21 cells were pretreated with various concentrations of Mn^{2+}, and then the Marc-145 cells were infected with two PRRSV strains, whereas the 3D4/21 cells were infected with VSV and HSV-1. As shown in Fig. 1A and B and Supplementary Fig. S2A, Mn^{2+} inhibited PRRSV XJ17-5 replications in Marc-145 cells in a dose-dependent manner at both 24 h and 48 h post infections, as evidenced by Western blotting, GFP fluorescence and TCID50 assay. Similarly, the Mn^{2+} treatment showed comparable anti-PRRSV JXA1-R-GFP effect (Fig. 1C and D and Fig. S2B). On the other hand, the VSV replication in 3D4/21 cells in the presence of various concentrations of Mn^{2+} was examined, and the results revealed that Mn^{2+} suppressed VSV replication in a dose dependent manner in Western blotting, fluorescence microscopy and TCID50 assay (Fig. 1E and F and Fig. S2C). Further, HSV-1 replication in 3D4/21 cells was also decreased in a dose-dependent manner after the pretreatment with Mn^{2+} (Fig. 1G and H and Fig. S2D).

 doi:10.20944/preprints202302.0099.v1

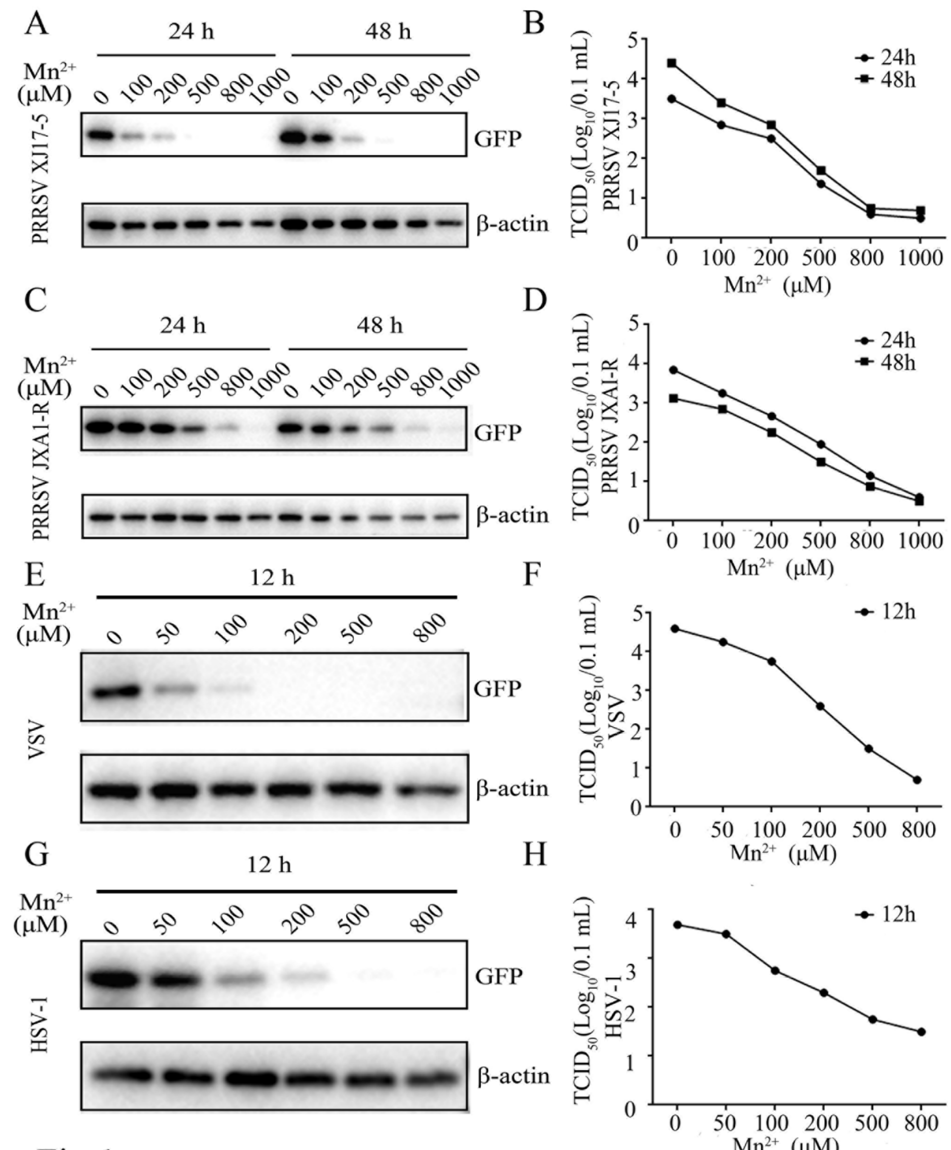

Fig 1

Figure 1. Mn^{2+} exerts antiviral functions against PRRSV, VSV, and HSV-1. (A-D) Marc-145 cells were pretreated with Mn^{2+} (0, 100, 200, 500, 800, 1000 μM) for 24 h, and then infected with 0.1 MOI HP-PRRSV-GFP XJ17-5 (A and B) or HP-PRRSV-GFP JXA1-R (C and D) for 24 h and 48 h, respectively. (E-H) 3D4/21 cells were pretreated with Mn^{2+} (0, 50, 100, 200, 500, 800 μM) for 24 h, and then infected with 0.001 MOI VSV-GFP (E and F) or 0.01 MOI HSV-1-GFP (G and H) for 12 h. The GFP and β-actin protein levels were detected using Western blot analysis (A, C, E, G), and the virus titers in the supernatants were examined by TCID50 assay (B, D, F, H).

3.2. Mn^{2+} triggered antiviral activity against PRRSVs was cGAS-STING independent

Mn^{2+} has been found to promote the sensitivity of the cGAS-STING pathway for double-stranded DNA [16]. Thus, we first explored whether Mn^{2+} affects PRRSV replications depending on cGAS and STING. The $cGAS^{-/-}$ Marc-145 cells (Fig. S1A) and $STING^{-/-}$ Marc-145 cells were both utilized for PRRSV infections in the presence of Mn^{2+}, and the anti-PRRSV activity by Mn^{2+} was examined. Western blotting and TCID50 assay showed that PRRSV XJ17-5 replication was upregulated in $cGAS^{-/-}$ Marc-145 cells relative to those in normal Marc-145 cells. However, Mn^{2+} triggered anti-PRRSV XJ17-5 activity did not appear altered in $cGAS^{-/-}$ Marc-145 cells at both 24 h and 48 h post infections (Fig. 2A and B). Similar results were obtained with the infections of PRRSV JXA1-R (Fig. 2C and D).

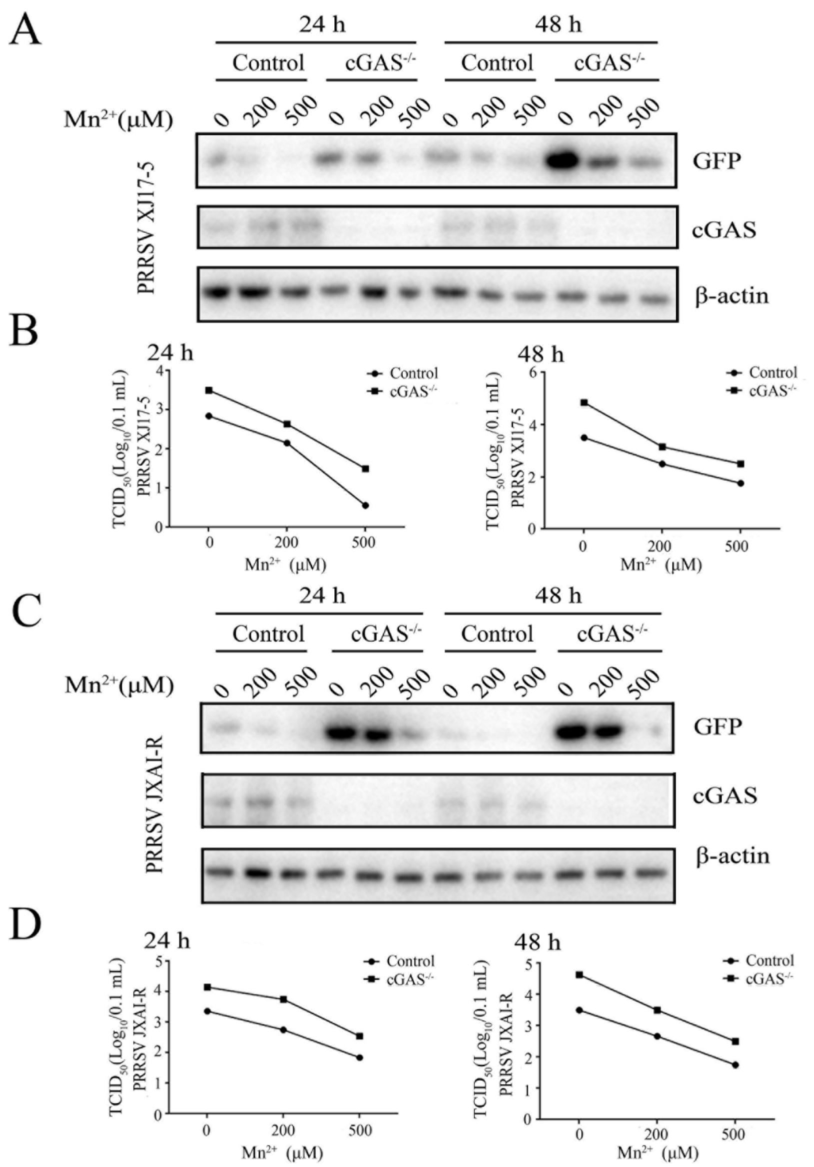

Figure 2. Mn^{2+} mediates antiviral functions against PRRSV in the cGAS-independent manner. The cGAS$^{-/-}$ Marc-145 cells and normal Marc-145 control cells were pretreated with Mn^{2+} (0, 200, 500 μM) for 24 h, and then infected with 0.1 MOI HP-PRRSV XJ17-5 (A and B) or 0.1 MOI PRRSV JXA1-R (C and D) for 24 h and 48 h, respectively. The cell samples were collected and subjected to Western blot analysis using anti-GFP, anti-cGAS and anti-β-actin (A and C). The virus titers in the supernatants were detected using TCID50 assay (B and D).

Further, the effect of Mn^{2+} on PRRSV replication was examined in STING$^{-/-}$ Marc-145 cells. Western blotting and TCID50 assay showed that the PRRSV XJ17-5 replication was upregulated in STING$^{-/-}$ Marc-145 cells relative to normal Marc-145 cells. However, the Mn^{2+} triggered anti-PRRSV XJ17-5 activity was retained at both 24 h and 48 h post infections (Fig. 3A and B). Similar results were obtained with the PRRSV JXA1-R infections (Fig. 3C and D). Together, the results indicated that although the cGAS-STING pathway plays a role in the anti-PRRSV innate immunity, it is not required for Mn^{2+} triggered anti-PRRSV activity.

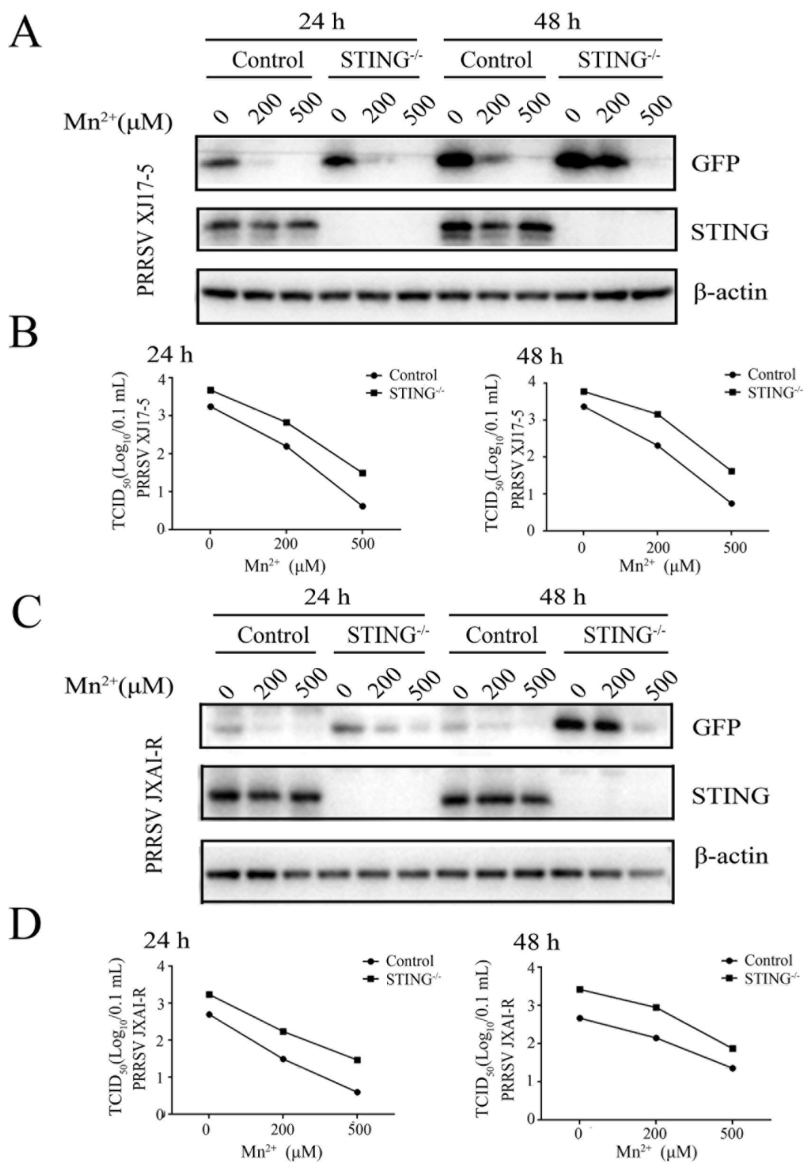

Figure 3. Mn^{2+} mediates antiviral functions against PRRSV in the STING-independent manner.The $STING^{-/-}$ Marc-145 cells and normal Marc-145 control cells were pretreated with Mn^{2+} (0, 200, 500 μM) for 24 h, and then infected with 0.1 MOI HP-PRRSV XJ17-5 (A and B) or 0.1 MOI PRRSV JXA1-R (C and D) for 24 h and 48 h, respectively. The cell samples were collected and subjected to Western blot analysis using anti-GFP, anti-STING and anti-β-actin (A and C). The virus titers in the supernatants were detected using TCID50 assay (B and D).

3.3. Mn^{2+} triggered antiviral activity against VSV and HSV-1 was independent of cGAS-STING

To detect whether the antiviral functions of Mn^{2+} against VSV and HSV-1 in 3D4/21 cells were dependent on cGAS and STING, the $cGAS^{-/-}$ 3D4/21 cells (Fig. S1B) and $STING^{-/-}$ 3D4/21 cells were both examined after virus infections. The results showed that the replications of VSV and HSV-1 were both upregulated in $cGAS^{-/-}$ 3D4/21 cells compared with those in normal 3D4/21 cells. However, the antiviral functions of Mn^{2+} were not attenuated in $cGAS^{-/-}$ 3D4/21 cells as evidenced by Western blotting and TCID50 assay (Fig. 4A-D). On the other hand, the VSV and HSV-1 replications were also upregulated in $STING^{-/-}$ 3D4/21 cells compared with those in normal 3D4/21 cells, but the Mn^{2+} triggered antiviral activities were not diminished in $STING^{-/-}$ 3D4/21 cells (Fig. 5A-D). Again and all together, the results clearly suggested that the cGAS-STING pathway is not essential for Mn^{2+} triggered antiviral functions despite that it plays an important role in the antiviral innate immunity.

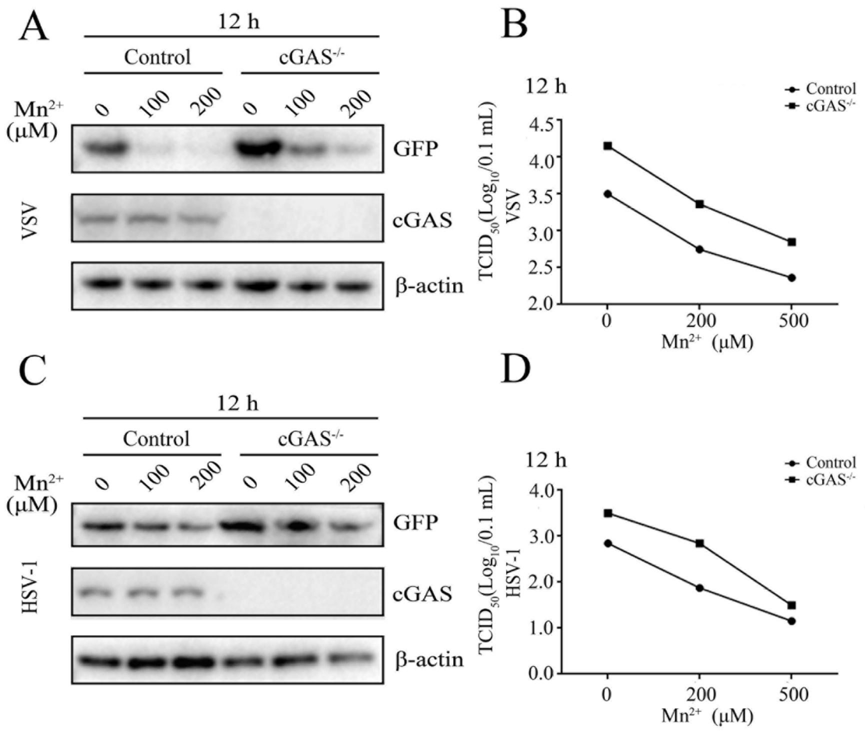

Figure 4. Mn^{2+} mediates antiviral functions against VSV and HSV-1 in the cGAS-independent manner. (A-B) $cGAS^{-/-}$ 3D4/21 cells and normal 3D4/21 control cells were pretreated with Mn^{2+} (0, 100, 200 μM) for 24 h, and then infected with 0.001 MOI VSV for 12 h. (C-D) $cGAS^{-/-}$ 3D4/21 cells and normal 3D4/21 cells were pretreated with Mn^{2+} (0, 100, 200 μM) for 24 h, and subsequently infected with 0.01 MOI HSV-1 for 12 h. The cell samples were collected and subjected to Western blot analysis using anti-GFP, anti-cGAS and anti-β-actin (A and C). The virus titers in the supernatants were detected using TCID50 assay (B and D).

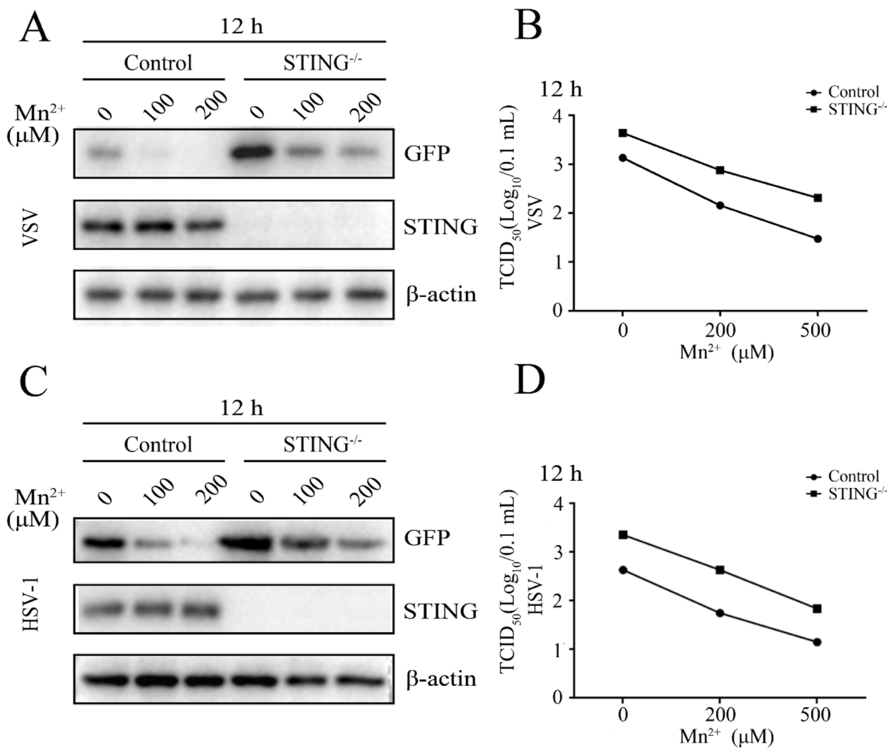

 doi:10.20944/preprints202302.0099.v1

Figure 5. Mn^{2+} mediates antiviral functions against VSV and HSV-1 in the STING-independent manner. (A-B) $STING^{-/-}$ 3D4/21 cells and normal 3D4/21 control cells were pretreated with Mn^{2+} (0, 100, 200 μM) for 24 h, and then infected with 0.001 MOI VSV for 12 h. (C-D) $STING^{-/-}$ 3D4/21 cells and normal 3D4/21 cells were pretreated with Mn^{2+} (0, 100, 200 μM) for 24 h, and subsequently infected with 0.01 MOI HSV-1 for 12 h. The cell samples were collected and subjected to Western blot analysis using anti-GFP, anti-STING and anti-β-actin (A and C). The virus titers in the supernatants were detected using TCID50 assay (B and D).

3.4. Mn^{2+} treatment promoted cGAS-STING signaling activity

To further validate whether Mn^{2+} can activate the cGAS-STING pathway, the effect of Mn^{2+} on the cGAS-STING signaling pathway was investigated in both 293T and 3D4/21 cells. In 293T cells, the co-transfection of porcine cGAS and STING activated downstream IFNβ and ISRE promoter activities as well as IFNβ and ISG60 gene transcriptions (Fig. 6A and B), whereas the Mn^{2+} treatments increased the two promoter activities and IFNβ and ISG60 transcriptions in dose dependent manners (Fig 6A and B). In 3D4/21 cells, both cGAS agonist polydA:dT and STING agonist 2’3’-cGAMP activated downstream IFNβ and ISG15 gene transcriptions, and the phosphorylations of TBK and IRF3 in Western blotting (Fig 6C and D). Similarly, Mn^{2+} further promoted the IFNβ and ISG15 transcriptions, and the phosphorylations of TBK and IRF3 in dose dependent manners (Fig 6C and D). The results suggested that the cGAS-STING activation may be one of the redundant mechanisms of Mn^{2+} triggered antiviral functions in cells.

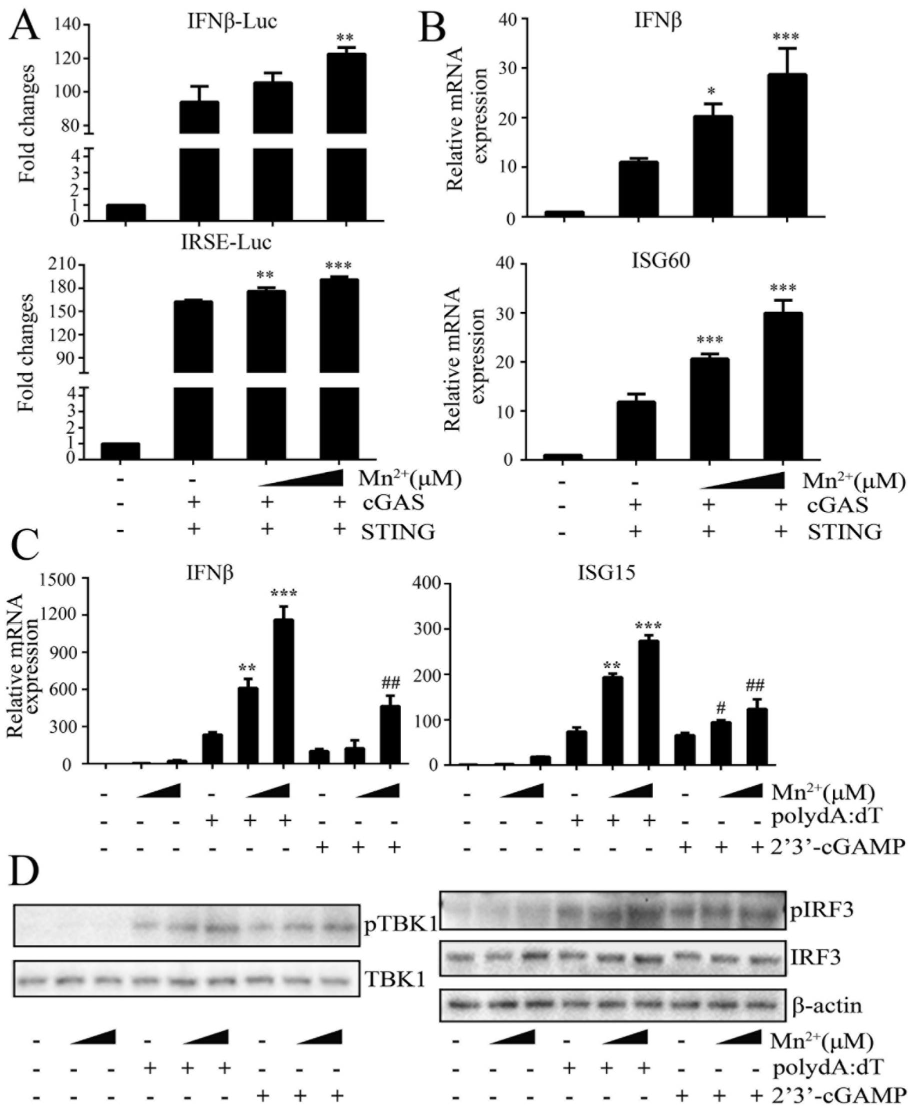

Figure 6. Mn^{2+} promotes cGAS-STING signaling activity. (A) HEK293T cells in 96-well plates were con-transfected with 20 ng cGAS-HA and 10 ng STING-GFP, plus 10 ng IFNβ-luc or ISRE-luc and 0.2 ng pRL-TK plasmid for 24 h. Cells were then treated with Mn^{2+} (0, 100, 200 μM) for 24 h, and the luciferase activities were examined. (B) HEK293T cells in 24-well plates were co-transfected with 400 ng cGAS-HA and 400 ng STING-GFP plasmids for 24 h. Cells were then exposed to Mn^{2+} (0, 100, 200 μM) for another 24 h, and subjected to RT-qPCR for downstream gene detection. (C-D) 3D4/21 cells in 24-well plates were transfected with polydA:dT (1 μg/mL) or 2'3'-cGAMP (2 μg/mL) for 8 h using lipofectiamine 2000. Twenty-four hours post transfection, cells were incubated with Mn^{2+} (0, 100, 200 μM) for another 24 h, and then downstream gene expressions were detected using RT-qPCR (C) and Western blot analysis with the indicated antibodies (D). * or #, $p < 0.05$. ** or ##, $p < 0.01$. ***, $p < 0.001$.

4. Discussion

The element Mn is critical for almost all forms of life [10-12]. Cytosolic Mn^{2+} has been reported to be involved in the dsDNA sensing activity of cGAS, and protects against DNA viruses [16]. Recent studies have shown that Mn^{2+} could directly activate cGAS, which was independent of dsDNA [17, 18]. In addition, the overlapping mechanisms between the antiviral innate immunity developed against RNA and DNA viruses have been reviewed previously [26]. Many RNA viruses of families *Flaviviridae*, *Coronaviridae*, and *Arteriviridae* have been found to be associated with the cGAS-STING pathway [19-22, 27]. Likewise, in our study, we demonstrated that Mn^{2+} exerts antiviral functions against a DNA virus (HSV-1) and some RNA viruses (PRRSV XJ17-5, PRRSV JXA1-R, and VSV) in a dose-dependent manner. The Mn^{2+} exhibited a broad antiviral activity, which is similar to that mediated by the cGAS-STING pathway. At the first glance, it is logical to deduce that Mn^{2+} exerts antiviral activity by acting on cGAS-STING signaling pathway. However, our further investigation revealed that Mn^{2+} triggered antiviral activity is cGAS-STING independent, suggesting there is other cell mechanism which mediates the Mn^{2+} antiviral functions.

Previously, Mn^{2+} has been found to participate in the phosphorylation of p53 [15, 28]. p53 is a tumor suppressor gene, and functions most commonly in cell cycle arrest, differentiation as well as apoptosis [29]. Moreover, p53 has been reported to be involved the regulation of antiviral functions [30-32]. For example, p53 overexpression represses HIV-1 long terminal repeat (LTR) transcriptional elongation via preventing the phosphorylation of serine 2 of the pol II C-terminal domain (CTD), resulting in the inhibition of HIV-1 transcription and replication [30]. Influenza virus infection promotes the activation of the p53 pathway leading to apoptosis, and suppression of p53 activity contributes to influenza virus infection [31]. Similarly, depletion of p53 was shown to promote porcine epidemic diarrhea virus (PEDV) infection susceptibility [32]. p53 has robust antiviral immunity by activation of the IFN pathway and the induction of several antiviral proteins [33, 34]. Miciak *et al* have identified that p53 contributes to perpetuate IFN signaling through ISG-dependent positive feedback loops [35]. Then, Hao *et al* have discovered that p53 facilitates IFN signaling and secretion, and activates ISREs and ISG expression during viral infection [32].

In addition, a recent report found that Mn^{2+} alone activates phosphorylation of TBK1 with ATM involved, and enhances DNA- or RNA-mediated innate immune responses [36]. TBK1 is the downstream mediator of multiple DNA sensors, such as Ku70, IFI16, cGAS, and DDX41 [37]. Similarly, it is also involved in the signaling pathway of RNA sensors, such as RIG-I and MDA5 [38, 39]. Here, our study demonstrates that Mn^{2+} has antiviral functions against RNA viruses (PRRSVs, VSV) and a DNA virus (HSV-1) in $cGAS^{-/-}$ and $STING^{-/-}$ cells. Mn^{2+} may initiate ATM-TBK1 signaling to exert its broad spectrum antiviral functions [36]. Together, we speculate that Mn^{2+} may induce activation of p53 and/or ATM-TBK1 to establish a powerfully antiviral state through cGAS-STING independent signaling pathways.

Nevertheless, we observed that the cGAS-STING signaling is indeed activated by the Mn^{2+} treatment. This observation is consistent with the previous discovery that Mn^{2+} suppressed virus replications through sensitizing both cGAS and STING [16] and suggests that cGAS-STING is one of the cell machinery that mediates Mn^{2+} antiviral functions. In our study, although Mn^{2+} mediated antiviral functions via a cGAS-STING independent pathway, it was also identified to promote cGAS-STING signaling activity. Then, what is the relationship between cGAS-STING signaling and other cell machinery triggered by the Mn^{2+}? These cell machineries must be redundant, and together participate in the Mn^{2+} triggered antiviral functions. However, the exact molecular mechanisms underlying Mn^{2+} mediated antiviral functions deserve further exploration for a complete elucidation.

In summary, we demonstrated that Mn^{2+} inhibits PRRSV XJ17-5, PRRSV JXA1-R, VSV, and HSV-1 replications in a cGAS-STING independent manner. Our results reveal that Mn^{2+} may harbor multiple cellular mechanisms to exert its broad spectrum antiviral activity, and suggest that the Mn^{2+} has the potential to be used not only as an antiviral therapeutics but also as the immune adjuvant in some animal vaccines.

Conflicts of Interest statement: The authors declare no any potential conflict of interest

Author Contributions statement: J.Z and Z.L conceived and designed the experiments; S.S, Y.X, M.Q, S.J, Q.C, J.L performed the experiments; T.Z, N.C, W.Z, F.M analyzed the data; S.S and J.Z wrote the paper. All authors contributed to the article and approved the submitted version.

Acknowledgments: The work was partly supported by the National Natural Science Foundation of China (32172867; 32202818), the 111 Project D18007, and A Project Funded by the Priority Academic Program Development of Jiangsu Higher Education Institutions (PAPD).

References

1. Takeuchi, O.; Akira, S., Pattern recognition receptors and inflammation. *Cell* **2010,** 140, (6), 805-20.
2. Cui, J.; Chen, Y.; Wang, H. Y.; Wang, R. F., Mechanisms and pathways of innate immune activation and regulation in health and cancer. *Hum Vaccin Immunother* **2014,** 10, (11), 3270-85.
3. Roers, A.; Hiller, B.; Hornung, V., Recognition of Endogenous Nucleic Acids by the Innate Immune System. *Immunity* **2016,** 44, (4), 739-54.
4. Briard, B.; Place, D. E.; Kanneganti, T. D., DNA Sensing in the Innate Immune Response. *Physiology (Bethesda)* **2020,** 35, (2), 112-124.
5. Chen, N.; Xia, P.; Li, S.; Zhang, T.; Wang, T. T.; Zhu, J., RNA sensors of the innate immune system and their detection of pathogens. *IUBMB Life* **2017,** 69, (5), 297-304.
6. Hopfner, K. P.; Hornung, V., Molecular mechanisms and cellular functions of cGAS-STING signalling. *Nat Rev Mol Cell Biol* **2020,** 21, (9), 501-521.
7. Sun, L.; Wu, J.; Du, F.; Chen, X.; Chen, Z. J., Cyclic GMP-AMP synthase is a cytosolic DNA sensor that activates the type I interferon pathway. *Science* **2013,** 339, (6121), 786-91.
8. Zhang, X.; Bai, X. C.; Chen, Z. J., Structures and Mechanisms in the cGAS-STING Innate Immunity Pathway. *Immunity* **2020,** 53, (1), 43-53.
9. Balka, K. R.; Louis, C.; Saunders, T. L.; Smith, A. M.; Calleja, D. J.; D'Silva, D. B.; Moghaddas, F.; Tailler, M.; Lawlor, K. E.; Zhan, Y.; Burns, C. J.; Wicks, I. P.; Miner, J. J.; Kile, B. T.; Masters, S. L.; De Nardo, D., TBK1 and IKKepsilon Act Redundantly to Mediate STING-Induced NF-kappaB Responses in Myeloid Cells. *Cell Rep* **2020,** 31, (1), 107492.
10. Horning, K. J.; Caito, S. W.; Tipps, K. G.; Bowman, A. B.; Aschner, M., Manganese Is Essential for Neuronal Health. *Annu Rev Nutr* **2015,** 35, 71-108.
11. Kwakye, G. F.; Paoliello, M. M.; Mukhopadhyay, S.; Bowman, A. B.; Aschner, M., Manganese-Induced Parkinsonism and Parkinson's Disease: Shared and Distinguishable Features. *Int J Environ Res Public Health* **2015,** 12, (7), 7519-40.
12. Aschner, M., Manganese: brain transport and emerging research needs. *Environ Health Perspect* **2000,** 108 Suppl 3, (Suppl 3), 429-32.
13. Bryan, M. R.; Uhouse, M. A.; Nordham, K. D.; Joshi, P.; Rose, D. I. R.; O'Brien, M. T.; Aschner, M.; Bowman, A. B., Phosphatidylinositol 3 kinase (PI3K) modulates manganese homeostasis and manganese-induced cell signaling in a murine striatal cell line. *Neurotoxicology* **2018,** 64, 185-194.
14. Bryan, M. R.; Bowman, A. B., Manganese and the Insulin-IGF Signaling Network in Huntington's Disease and Other Neurodegenerative Disorders. *Adv Neurobiol* **2017,** 18, 113-142.
15. Tidball, A. M.; Bryan, M. R.; Uhouse, M. A.; Kumar, K. K.; Aboud, A. A.; Feist, J. E.; Ess, K. C.; Neely, M. D.; Aschner, M.; Bowman, A. B., A novel manganese-dependent ATM-p53 signaling pathway is selectively impaired in patient-based neuroprogenitor and murine striatal models of Huntington's disease. *Hum Mol Genet* **2015,** 24, (7), 1929-44.
16. Wang, C.; Guan, Y.; Lv, M.; Zhang, R.; Guo, Z.; Wei, X.; Du, X.; Yang, J.; Li, T.; Wan, Y.; Su, X.; Huang, X.; Jiang, Z., Manganese Increases the Sensitivity of the cGAS-STING Pathway for Double-Stranded DNA and Is Required for the Host Defense against DNA Viruses. *Immunity* **2018,** 48, (4), 675-687 e7.
17. Zhao, Z.; Ma, Z.; Wang, B.; Guan, Y.; Su, X. D.; Jiang, Z., Mn(2+) Directly Activates cGAS and Structural Analysis Suggests Mn(2+) Induces a Noncanonical Catalytic Synthesis of 2'3'-cGAMP. *Cell Rep* **2020,** 32, (7), 108053.
18. Hooy, R. M.; Massaccesi, G.; Rousseau, K. E.; Chattergoon, M. A.; Sohn, J., Allosteric coupling between Mn2+ and dsDNA controls the catalytic efficiency and fidelity of cGAS. *Nucleic Acids Res* **2020,** 48, (8), 4435-4447.
19. Yu, P.; Miao, Z.; Li, Y.; Bansal, R.; Peppelenbosch, M. P.; Pan, Q., cGAS-STING effectively restricts murine norovirus infection but antagonizes the antiviral action of N-terminus of RIG-I in mouse macrophages. *Gut Microbes* **2021,** 13, (1), 1959839.
20. Iampietro, M.; Dumont, C.; Mathieu, C.; Spanier, J.; Robert, J.; Charpenay, A.; Dupichaud, S.; Dhondt, K. P.; Aurine, N.; Pelissier, R.; Ferren, M.; Mely, S.; Gerlier, D.; Kalinke, U.; Horvat, B., Activation of cGAS/STING pathway upon paramyxovirus infection. *iScience* **2021,** 24, (6), 102519.
21. Webb, L. G.; Veloz, J.; Pintado-Silva, J.; Zhu, T.; Rangel, M. V.; Mutetwa, T.; Zhang, L.; Bernal-Rubio, D.; Figueroa, D.; Carrau, L.; Fenutria, R.; Potla, U.; Reid, S. P.; Yount, J. S.; Stapleford, K. A.; Aguirre, S.; Fernandez-Sesma, A., Chikungunya virus antagonizes cGAS-STING mediated type-I interferon responses by degrading cGAS. *PLoS Pathog* **2020,** 16, (10), e1008999.
22. Xu, Y.; Zhang, Y.; Sun, S.; Luo, J.; Jiang, S.; Zhang, J.; Liu, X.; Shao, Q.; Cao, Q.; Zheng, W.; Chen, N.; Meurens, F.; Zhu, J., The Innate Immune DNA Sensing cGAS-STING Signaling Pathway Mediates Anti-PRRSV Function. *Viruses* **2021,** 13, (9).
23. Chen, N.; Li, S.; Li, X.; Ye, M.; Xiao, Y.; Yan, X.; Li, X.; Zhu, J., The infectious cDNA clone of commercial HP-PRRS JXA1-R-attenuated vaccine can be a potential effective live vaccine vector. *Transbound Emerg Dis* **2020**.
24. Li, S.; Yang, J.; Zhu, Y.; Ji, X.; Wang, K.; Jiang, S.; Luo, J.; Wang, H.; Zheng, W.; Chen, N.; Ye, J.; Meurens, F.; Zhu, J., Chicken DNA Sensing cGAS-STING Signal Pathway Mediates Broad Spectrum Antiviral Functions. *Vaccines (Basel)* **2020,** 8, (3).
25. Jiang, S.; Luo, J.; Zhang, Y.; Cao, Q.; Wang, Y.; Xia, N.; Zheng, W.; Chen, N.; Meurens, F.; Wu, H.; Zhu, J., The Porcine and Chicken Innate DNA Sensing cGAS-STING-IRF Signaling Axes Exhibit Differential Species Specificity. *J Immunol* **2022,** 209, (2), 412-426.
26. Cai, C.; Tang, Y. D.; Xu, G.; Zheng, C., The crosstalk between viral RNA- and DNA-sensing mechanisms. *Cell Mol Life Sci* **2021,** 78, (23), 7427-7434.

doi:10.20944/preprints202302.0099.v1

27. Ma, Z.; Damania, B., The cGAS-STING Defense Pathway and Its Counteraction by Viruses. *Cell Host Microbe* **2016,** 19, (2), 150-8.
28. Chan, D. W.; Son, S. C.; Block, W.; Ye, R.; Khanna, K. K.; Wold, M. S.; Douglas, P.; Goodarzi, A. A.; Pelley, J.; Taya, Y.; Lavin, M. F.; Lees-Miller, S. P., Purification and characterization of ATM from human placenta. A manganese-dependent, wortmannin-sensitive serine/threonine protein kinase. *The Journal of biological chemistry* **2000,** 275, (11), 7803-10.
29. Muller, P. A.; Vousden, K. H., Mutant p53 in cancer: new functions and therapeutic opportunities. *Cancer cell* **2014,** 25, (3), 304-17.
30. Mukerjee, R.; Claudio, P. P.; Chang, J. R.; Del Valle, L.; Sawaya, B. E., Transcriptional regulation of HIV-1 gene expression by p53. *Cell Cycle* **2010,** 9, (22), 4569-78.
31. Turpin, E.; Luke, K.; Jones, J.; Tumpey, T.; Konan, K.; Schultz-Cherry, S., Influenza virus infection increases p53 activity: role of p53 in cell death and viral replication. *J Virol* **2005,** 79, (14), 8802-11.
32. Hao, Z.; Fu, F.; Cao, L.; Guo, L.; Liu, J.; Xue, M.; Feng, L., Tumor suppressor p53 inhibits porcine epidemic diarrhea virus infection via interferon-mediated antiviral immunity. *Mol Immunol* **2019,** 108, 68-74.
33. Munoz-Fontela, C.; Macip, S.; Martinez-Sobrido, L.; Brown, L.; Ashour, J.; Garcia-Sastre, A.; Lee, S. W.; Aaronson, S. A., Transcriptional role of p53 in interferon-mediated antiviral immunity. *The Journal of experimental medicine* **2008,** 205, (8), 1929-38.
34. Munoz-Fontela, C.; Pazos, M.; Delgado, I.; Murk, W.; Mungamuri, S. K.; Lee, S. W.; Garcia-Sastre, A.; Moran, T. M.; Aaronson, S. A., p53 serves as a host antiviral factor that enhances innate and adaptive immune responses to influenza A virus. *J Immunol* **2011,** 187, (12), 6428-36.
35. Miciak, J.; Bunz, F., Long story short: p53 mediates innate immunity. *Biochimica et biophysica acta* **2016,** 1865, (2), 220-7.
36. Sui, H.; Chen, Q.; Yang, J.; Srirattanapirom, S.; Imamichi, T., Manganese enhances DNA- or RNA-mediated innate immune response by inducing phosphorylation of TANK-binding kinase 1. *iScience* **2022,** 25, (11), 105352.
37. Zhou, R.; Zhang, Q.; Xu, P., TBK1, a central kinase in innate immune sensing of nucleic acids and beyond. *Acta biochimica et biophysica Sinica* **2020,** 52, (7), 757-767.
38. Rehwinkel, J.; Gack, M. U., RIG-I-like receptors: their regulation and roles in RNA sensing. *Nature reviews. Immunology* **2020,** 20, (9), 537-551.
39. Yoneyama, M.; Fujita, T., RNA recognition and signal transduction by RIG-I-like receptors. *Immunological reviews* **2009,** 227, (1), 54-65.